

An Efficient Algorithm for Sum-Rate Maximization in Fluid Antenna-Assisted ISAC System

Qian Zhang, *Graduate Student Member, IEEE*, Mingjie Shao, *Member, IEEE*, Tong Zhang, *Member, IEEE*, Gaojie Chen, *Senior Member, IEEE*, and Ju Liu, *Senior Member, IEEE*

Abstract—In this letter, we investigate the fluid antenna (FA)-assisted integrated sensing and communication (ISAC) system, where communication and radar sensing employ the co-waveform design. Specifically, we focus on the beamformer design and antenna position configuration to realize a higher communication rate while guaranteeing the minimum radar probing power. Different from existing beamformer algorithms, we propose an efficient proximal distance algorithm (PDA) to solve the multiuser sum-rate maximization problem with radar sensing constraint to obtain the closed-form beamforming vector. In addition, we develop an extrapolated projected gradient (EPG) algorithm to obtain a better antenna location configuration for FA to enhance the ISAC performance. Numerical results show that the considered FA-assisted ISAC system enjoys a higher sum-rate by the proposed algorithm, compared with that in existing non-FA ISAC systems.

Index Terms—Fluid antenna, integrated sensing and communication, sum-rate maximization, proximal distance algorithm

I. INTRODUCTION

INTEGRATED sensing and communication (ISAC) is recognized as a promising technology for next-generation wireless networks [1]–[4]. ISAC has received extensive attention: symbol-level ISAC [5], [6], ISAC waveform design [3], [4], [7], [8], receive filter design for multiple-input multiple-output (MIMO) [9], [10], Cramér-Rao bound optimization [11], [12], etc. In these studies, the MIMO technique plays a vital role due to its precoding capability for beamforming and waveform shaping. As the size of MIMO increases, ISAC systems will receive more performance gains. In [7], Liu *et al.* employed the fractional programming (FP) algorithm in [13] and successive convex approximation (SCA) algorithm to solve the sum-rate maximization problem with sensing power constraint. In [8], Wang *et al.* proposed a relaxed method and used the semi-definite relaxation (SDR) algorithm to solve the communication and sensing trade-off design problem. These optimization algorithms unfortunately have high complexity, especially as the size of MIMO increases.

This work was supported in part by the National Natural Science Foundation of China under Grant 62071275; in part by the Key R&D Plan of Shandong Province of China under Grant 2021SFGC0701; in part by the Natural Science Foundation of Shandong Province of China under Grant ZR2023QF103. The corresponding authors: Ju Liu and Mingjie Shao. E-mail: {juliu, mingjieshao}@sdu.edu.cn.

Qian Zhang, Mingjie Shao, and Ju Liu are with School of Information Science and Engineering, Shandong University, Qingdao 266237, China (qianzhang2021@mail.sdu.edu.cn; {mingjieshao, juliu}@sdu.edu.cn).

Tong Zhang is with the Institute of Intelligent Ocean Engineering, Harbin Institute of Technology (Shenzhen), Shenzhen, 518055, China (zhangt77@jnu.edu.cn).

Gaojie Chen is with 5GIC & 6GIC, Institute for Communication Systems, University of Surrey, Guildford GU2 7XH, UK (gaojie.chen@surrey.ac.uk).

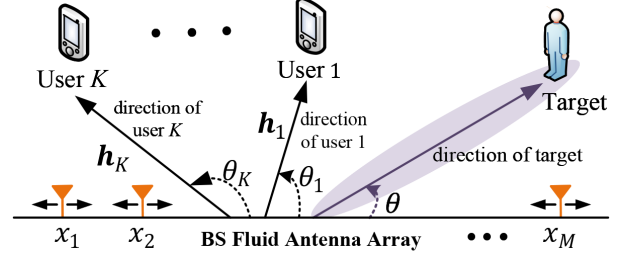


Fig. 1. The model of fluid antenna-assisted ISAC system.

Recently, fluid antennas (FAs) have been proposed to further enhance the MIMO performance by locally moving the antenna position to reconfigure properties such as polarization and radiation pattern [14], [15]. FA systems can use fewer radio frequency (RF) links to achieve better performance than traditional MIMO by moving antenna positions. FA has been demonstrated to have significant effects in enhancing MIMO communications [16], [17], beamforming [18], [19], mobile edge computing [20], index modulation [21], over-the-air computation [22], etc. Owing to these advantages, FA will bring more performance improvement for ISAC. At present, FA-assisted ISAC problems are rarely explored. The work [23] adopted deep reinforcement learning (DRL) to address FA-assisted ISAC problems, while DRL consumes a large amount of training data and time.

In this paper, we investigate the deployment and optimization of FAs at the base station (BS) for ISAC, where a canonical sum-rate maximization problem with radar sensing constraint for beamformer optimization is considered. Unlike the existing ISAC algorithms, we propose an efficient proximal distance algorithm (PDA) to derive the closed-form beamformer. Also, an extrapolated projected gradient (EPG) algorithm is proposed for the configuration of FA position. Numerical results show that the proposed algorithm can achieve better performance than existing algorithms. The case study of optimal solutions exhibits that FA can significantly improve ISAC performance by selecting the preferable channel.

II. SYSTEM MODEL

We consider a downlink transmission in an FA-assisted ISAC system, as shown in Fig. 1. The BS, which has M FAs, serves K single-antenna users and senses a point-like target at the same time. We assume that FAs can move in a one-dimensional (1D) line segment of length D . We denote $x_m \in [0, D]$ as the m th FA's position and the assembled

vector $\mathbf{x} = [x_1, x_2, \dots, x_M] \in \mathbb{R}^M$ as the antenna position vector (APV). In such an ISAC system, the transmitted signal is a dual-functional waveform for both radar sensing and communication. The channel from the BS to the k th user is modeled by the following line-of-sight (LoS) model, which is given by

$$\mathbf{h}_k = \sigma_k \mathbf{a}(\mathbf{x}, \theta_k), \quad k = 1, 2, \dots, K, \quad (1)$$

where σ_k and θ_k represent the channel propagation gain and angle of departure (AOD) of user k , respectively; $\mathbf{a}(\mathbf{x}, \theta_k) = [e^{jv_k x_1}, e^{jv_k x_2}, \dots, e^{jv_k x_M}]^T$, $v_k = \frac{2\pi}{\lambda} \cos(\theta_k)$ and λ is the wavelength. We employ a linear beamformer, where the transmitted signal at the BS is given by

$$\mathbf{x}_t = \sum_{k=1}^K \mathbf{w}_k s_k, \quad (2)$$

where \mathbf{w}_k is the beamformer for user k ; the signal s_k is the data symbol for user k and $s_k \sim \mathcal{CN}(0, 1)$. Then, the received signal y_k at user k is given by

$$y_k = \mathbf{h}_k^H \mathbf{x}_t + n_k, \quad k = 1, 2, \dots, K, \quad (3)$$

where $n_k \sim \mathcal{CN}(0, \sigma^2)$ denotes the additive white complex Gaussian noise at user k . The signal-to-interference-plus-noise ratio (SINR) of user k is given by

$$\gamma_k = \frac{|\mathbf{h}_k^H \mathbf{w}_k|^2}{\sum_{i=1, i \neq k}^K |\mathbf{h}_k^H \mathbf{w}_i|^2 + \sigma^2}, \quad k = 1, 2, \dots, K. \quad (4)$$

In the considered ISAC system, the transmitted signal should also sense a target in the interested direction [24]. This requires the ISAC system to provide sufficient pulse power along the target direction. To describe, the covariance matrix of transmitted signal \mathbf{x}_t is given by

$$\mathbf{R}_w = \mathbb{E}[\mathbf{x}_t \mathbf{x}_t^H] = \mathbf{W} \mathbf{W}^H,$$

where $\mathbf{W} = [\mathbf{w}_1, \mathbf{w}_2, \dots, \mathbf{w}_M]$. The power of the probing signal in the target direction can be expressed as [4], [8]

$$P(\mathbf{W}, \mathbf{x}, \theta) = \mathbf{a}^H(\mathbf{x}, \theta) \mathbf{R}_w \mathbf{a}(\mathbf{x}, \theta), \quad (5)$$

where θ denotes the angle of the target direction.

III. BEAMFORMER AND APV OPTIMIZATION

We aim to optimize the beamformer and APV to maximize the multiuser sum-rate while the radar probing power in the target direction is above a prefixed level. The joint design problem is mathematically formulated as

$$\max_{\mathbf{W}, \mathbf{x}} \sum_{k=1}^K \log_2(1 + \gamma_k(\mathbf{W}, \mathbf{x})) \quad (6a)$$

$$\text{s.t. } \mathcal{C}_{\text{BS}} : \sum_{k=1}^K \|\mathbf{w}_k\|_2^2 \leq P_{\text{max}}, \quad (6b)$$

$$\mathcal{C}_t : P(\mathbf{W}, \mathbf{x}, \theta) \geq P_t, \quad (6c)$$

$$\mathcal{C}_{\text{FR}} : x_1 \geq 0, \quad x_M \leq D, \quad (6d)$$

$$\mathcal{C}_{\text{AC}} : x_m - x_{m-1} \geq D_0, \quad m = 2, 3, \dots, M. \quad (6e)$$

In problem (6), the constraint (6b) is the power budget at the BS; the constraint (6c) requires the probing power to be

no less than a given threshold P_t ; constraints (6d) and (6e) restrict the FA positions in the interval $[0, D]$ and make sure the inter-antenna spacing is no less than D_0 , respectively.

Note that problem (6) is highly nonconvex with respect to the design parameters (\mathbf{W}, \mathbf{x}) . Plus, the design of FA positions amounts to the optimization of the unit circle manifold. These properties make problem (6) difficult to solve.

Our way of handling problem (6) is by the block successive upper bound minimization (BSUM) method. Following the same vein of the weighted minimum mean-square error (WMMSE) method [25]–[27], we can equivalently transform problem (6) into the following form

$$\min_{\mathbf{w}, \mathbf{x}, \mathbf{u}, \rho} \mathcal{F}(\mathbf{w}, \mathbf{x}, \mathbf{u}, \rho) \quad \text{s.t. } \mathcal{C}_{\text{BS}}, \mathcal{C}_{\text{FR}}, \mathcal{C}_{\text{AC}}, \mathcal{C}_t, \quad (7)$$

where

$$\mathcal{F}(\mathbf{w}, \mathbf{x}, \mathbf{u}, \rho) = \sum_{k=1}^K [w_k^H \mathbf{A}(\mathbf{x}) \mathbf{w}_k - 2\Re\{\mathbf{b}_k(\mathbf{x})^H \mathbf{w}_k\}]$$

with $\mathbf{u} \in \mathbb{C}^K$ and $\rho \in \mathbb{R}_{++}^K$ being introduced auxiliary variables, $\mathbf{A}(\mathbf{x}) = \sum_{k=1}^K \rho_k |u_k|^2 \mathbf{h}_k(\mathbf{x}) \mathbf{h}_k(\mathbf{x})^H$, $\mathbf{w} = [\mathbf{w}_1^T, \dots, \mathbf{w}_M^T]^T$, $\mathbf{b}_k(\mathbf{x}) = \rho_k^* u_k \mathbf{h}_k(\mathbf{x})$, and $\Re\{x\}$ denoting the real part of x . By leveraging the above transformation, we apply BSUM and obtain

$$\mathbf{u}^{\ell+1} = \arg \min_{\mathbf{u} \in \mathbb{C}^K} \mathcal{F}(\mathbf{w}^\ell, \mathbf{x}^\ell, \mathbf{u}, \rho^\ell); \quad (8a)$$

$$\rho^{\ell+1} = \arg \min_{\rho \in \mathbb{R}_{++}^K} \mathcal{F}(\mathbf{w}^\ell, \mathbf{x}^\ell, \mathbf{u}^{\ell+1}, \rho); \quad (8b)$$

$$\mathbf{w}^{\ell+1} = \arg \min_{\mathbf{w} \in \mathcal{C}_{\text{BS}} \cap \mathcal{C}_t} \mathcal{F}(\mathbf{w}, \mathbf{x}^\ell, \mathbf{u}^{\ell+1}, \rho^{\ell+1}); \quad (8c)$$

$$\mathbf{x}^{\ell+1} = \arg \min_{\mathbf{x} \in \mathcal{C}_t \cap \mathcal{C}_{\text{FR}} \cap \mathcal{C}_{\text{AC}}} \mathcal{F}(\mathbf{w}^{\ell+1}, \mathbf{x}, \mathbf{u}^{\ell+1}, \rho^{\ell+1}). \quad (8d)$$

Notably, the optimizations of \mathbf{u} in (8a) and ρ in (8b) have closed-form solutions, which are given by

$$u_k^{\ell+1} = \frac{(\mathbf{h}_k(\mathbf{x}^\ell))^H \mathbf{w}_k^\ell}{\sum_{i=1}^K |(\mathbf{h}_k(\mathbf{x}^\ell))^H \mathbf{w}_i^\ell|^2 + \sigma^2}, \quad (9)$$

$$\rho_k^{\ell+1} = (1 - (u_k^{\ell+1})^* (\mathbf{h}_k(\mathbf{x}^\ell))^H \mathbf{w}_k^\ell)^{-1},$$

for $k = 1, 2, \dots, K$, respectively; $(\cdot)^*$ denotes the complex conjugate.

However, the optimizations of beamformer \mathbf{w} and APV \mathbf{x} do not have closed forms. We custom-build efficient algorithms for these two subproblems.

A. Beamformer Optimization

To solve (8c), we consider the PDA [28], which approximates problem (8c) by

$$\min_{\mathbf{w}} \mathcal{F}(\mathbf{w}) + \bar{\rho} \cdot \text{dist}^2(\mathbf{w}, \mathcal{C}_{\text{BS}}) + \bar{\rho} \cdot \text{dist}^2(\mathbf{w}, \mathcal{C}_t), \quad (10)$$

where $\text{dist}(\mathbf{w}, \mathcal{X}) = \min_{\mathbf{y} \in \mathcal{X}} \|\mathbf{w} - \mathbf{y}\|_2$ is the distance function from a point \mathbf{w} to a set \mathcal{X} [28], [29]; $\bar{\rho} > 0$ is a given penalty parameter. Obviously, the problem (10) becomes close to the problem (8c) when $\bar{\rho}$ is large.

The distance function does not admit an explicit form. To address this issue, we majorize the distance function by

$$\text{dist}(\mathbf{w}, \mathcal{C}_{\text{BS}}) \leq \|\mathbf{w} - \tilde{\mathbf{w}}_{\text{BS}}\|_2, \quad \text{dist}(\mathbf{w}, \mathcal{C}_t) \leq \|\mathbf{w} - \tilde{\mathbf{w}}_t\|_2, \quad (11)$$

Algorithm 1 An Efficient PDA for Problem (8c)

- 1: **Input:** Initialize $\bar{\rho} > 0$, $\kappa > 1$, $i = 1$, $\mathbf{w}_k^0 = \mathbf{w}_k^1$, $k = 1, 2, \dots, K$.
 - 2: **Repeat:**
 - 3: $\mathbf{z}_k^i = \mathbf{w}_k^i + \frac{i-1}{i+2}(\mathbf{w}_k^i - \mathbf{w}_k^{i-1})$;
 - 4: $\mathbf{y}_k^i = \Pi_{\mathcal{C}_{\text{BS}}}(\mathbf{z}_k^i) + \Pi_{\mathcal{C}_t}(\mathbf{z}_k^i)$;
 - 5: $\mathbf{w}_k^{i+1} = (\mathbf{A} + 2\bar{\rho}\mathbf{I})^{-1}(\bar{\rho}\mathbf{y}_k^i + \mathbf{b}_k)$;
 - 6: Update $i = i + 1$;
 - 7: Update $\bar{\rho} = \kappa\bar{\rho}$ every I iterations;
 - 8: **Until** stopping criterion is satisfied.
-

where $\tilde{\mathbf{w}}_{\text{BS}} = \Pi_{\mathcal{C}_{\text{BS}}}(\mathbf{w})$, $\tilde{\mathbf{w}}_t = \Pi_{\mathcal{C}_t}(\mathbf{w})$, and the notation

$$\Pi_{\mathcal{C}_X}(\mathbf{y}) = \arg \min_{\mathbf{x} \in \mathcal{X}} \|\mathbf{x} - \mathbf{y}\|_2^2$$

is the projection of \mathbf{y} onto the set \mathcal{X} . One can show that

$$[\tilde{\mathbf{w}}_{\text{BS}}]_k = \begin{cases} \mathbf{w}_k, & \text{if } \|\mathbf{w}\|_2^2 \leq P_{\text{max}}, \\ \sqrt{P_{\text{max}}} \frac{\mathbf{w}_k}{\|\mathbf{w}\|_2}, & \text{otherwise,} \end{cases}$$

$$[\tilde{\mathbf{w}}_t]_k = \begin{cases} \mathbf{w}_k, & \text{if } \sum_{k=1}^K \mathbf{w}_k^H \mathbf{a}(\mathbf{x}, \theta) \mathbf{a}(\mathbf{x}, \theta)^H \mathbf{w}_k \geq P_t, \\ (\mathbf{I} - \mu \mathbf{a}(\mathbf{x}, \theta) \mathbf{a}(\mathbf{x}, \theta)^H)^{-1} \mathbf{w}_k, & \text{otherwise,} \end{cases}$$

where

$$\mu = \frac{1}{(\mathbf{a}(\mathbf{x}, \theta)^H \mathbf{a}(\mathbf{x}, \theta))^2} - \sqrt{\frac{\sum_{k=1}^K \xi_k^H \mathbf{a}(\mathbf{x}, \theta) \mathbf{a}(\mathbf{x}, \theta)^H \xi_k}{(\mathbf{a}(\mathbf{x}, \theta)^H \mathbf{a}(\mathbf{x}, \theta))^2 P_t}}.$$

The derivation of the closed-form projection $\tilde{\mathbf{w}}_t$ is shown in Appendix A.

By the distance majorization, at iteration \mathbf{w} , one only needs to solve an unconstrained quadratic programming problem, which is given by

$$\min_{\mathbf{w}} \mathcal{F}(\mathbf{w}) + \bar{\rho} \cdot (\|\mathbf{w} - \tilde{\mathbf{w}}_{\text{BS}}\|_2^2 + \|\mathbf{w} - \tilde{\mathbf{w}}_t\|_2^2). \quad (12)$$

It is worth mentioning that the optimal solution to the above problem has a closed form, which is given by

$$\mathbf{w}_k = (\mathbf{A} + 2\bar{\rho}\mathbf{I})^{-1} [\bar{\rho}([\tilde{\mathbf{w}}_{\text{BS}}]_k + [\tilde{\mathbf{w}}_t]_k) + \mathbf{b}_k]. \quad (13)$$

We summarized the PDA in Algorithm 1. Note that we also apply the extrapolation strategy, which was shown able to numerically accelerate the algorithmic convergence [30].

B. APV Optimization

In this section, we develop an EPG algorithm [31] to solve the problem (8d), which takes the following updates

$$\begin{aligned} \mathbf{x}^{i+1} &= \Pi_{\mathcal{C}_t \cap \mathcal{C}_{\text{FR}} \cap \mathcal{C}_{\text{AC}}}(\mathbf{z}^i - \eta \nabla_{\mathbf{x}} \mathcal{F}(\mathbf{z}^i | \mathbf{x}^i)), \\ \mathbf{z}^{i+1} &= \mathbf{x}^{i+1} + \zeta_{i+1}(\mathbf{x}^{i+1} - \mathbf{x}^i), \end{aligned} \quad (14)$$

where $\eta > 0$ is the descent step length, which is obtained by the backtracking line search [32] method; $\nabla_{\mathbf{x}} \mathcal{F}(\mathbf{z}^i | \mathbf{x}^i)$ denotes the gradient of \mathcal{F} at \mathbf{z}^i , and

$$\nabla_{\mathbf{x}} \mathcal{F}(\mathbf{x}) = \sum_{k=1}^K 2\sigma_k v_k \rho_k \text{diag}(\mathbf{h}_k^T) (u_k^* \mathbf{w}_k - |u_k|^2 \mathbf{R}_w \mathbf{h}_k);$$

Algorithm 2 A BSUM algorithm for Problem (6)

- 1: **Input:** Initialize \mathbf{W} , \mathbf{x} , and $\ell = 1$.
 - 2: **Repeat:**
 - 3: $u_k^{\ell+1} = \frac{(\mathbf{h}_k(\mathbf{x}^\ell))^H \mathbf{w}_k^\ell}{\sum_{i=1}^K |(\mathbf{h}_k(\mathbf{x}^\ell))^H \mathbf{w}_i^\ell|^2 + \sigma^2}$;
 - 4: $\rho_k^{\ell+1} = (1 - (u_k^{\ell+1})^* (\mathbf{h}_k(\mathbf{x}^\ell))^H \mathbf{w}_k^\ell)^{-1}$;
 - 5: Update $\mathbf{W}^{\ell+1}$ by PDA;
 - 6: Update $\mathbf{x}^{\ell+1}$ by EPG;
 - 7: Update $\ell = \ell + 1$;
 - 8: **Until** stopping criterion is satisfied.
-

the parameter $\zeta_{i+1} = \frac{\alpha_{i+1}-1}{\alpha_{i+1}}$, $\alpha_{i+1} = \frac{1+\sqrt{1+4\alpha_i^2}}{2}$ with $\alpha_1 = 0$; and $\Pi_{\mathcal{C}_t \cap \mathcal{C}_{\text{FR}} \cap \mathcal{C}_{\text{AC}}}$ can be obtained by solving the following problem

$$\min_{\mathbf{x}} \|\mathbf{x} - \boldsymbol{\kappa}\|_2^2 \quad \text{s.t. } \mathbf{x} \in \mathcal{C}_t \cap \mathcal{C}_{\text{FR}} \cap \mathcal{C}_{\text{AC}}, \quad (15)$$

where $\boldsymbol{\kappa}$ is a point to project.

However, problem (15) is non-convex due to the non-convex constraint \mathcal{C}_t . Then, we construct a concave quadratic surrogate function to minorize $\mathbf{a}(\mathbf{x}, \theta)^H \mathbf{R}_w \mathbf{a}(\mathbf{x}, \theta)$ as [19]

$$\mathbf{a}(\mathbf{x}, \theta)^H \mathbf{R}_w \mathbf{a}(\mathbf{x}, \theta) \geq g(\mathbf{x} | \bar{\mathbf{x}}) \triangleq \frac{1}{2} \mathbf{x}^T \mathbf{D} \mathbf{x} + \mathbf{d}^T \mathbf{x} + c, \quad (16)$$

where

$$\mathbf{D} = -2v^2 (\text{diag}(\mathbf{r}) - \mathbf{R}),$$

$$\begin{aligned} \mathbf{d}[n] &= 2v^2 \sum_{m=1}^M |R_{mn}| (\bar{x}_n - \bar{x}_m) - 2v \sum_{m=1}^M |R_{mn}| \sin(f(\bar{x}_n, \bar{x}_m)), \\ c &= \sum_{m=1}^M \sum_{n=1}^M |R_{mn}| [\cos(f(\bar{x}_n, \bar{x}_m)) + v \sin(f(\bar{x}_n, \bar{x}_m)) (\bar{x}_n - \bar{x}_m) \\ &\quad - \frac{1}{2} v^2 (\bar{x}_n - \bar{x}_m)^2], \end{aligned}$$

with $\mathbf{r} = [\sum_{m=1}^M |R_{m1}|, \sum_{m=1}^M |R_{m2}|, \dots, \sum_{m=1}^M |R_{mM}|]$, $v = \frac{2\bar{x}}{\chi} \cos(\theta)$, and $[\mathbf{R}]_{mn} = |R_{mn}|$, where $f(\bar{x}_n, \bar{x}_m) = v(\bar{x}_n - \bar{x}_m) + \angle R_{mn}$, $\bar{\mathbf{x}} = [\bar{x}_1, \bar{x}_2, \dots, \bar{x}_M]^T$, and R_{mn} is the element in the m th row and n th column of matrix \mathbf{R}_w for $n, m = 1, 2, \dots, M$; $\bar{\mathbf{x}}$ denotes any determined value for \mathbf{x} .

Therefore, the problem (15) is recast to

$$\min_{\mathbf{x}} \|\mathbf{x} - \boldsymbol{\kappa}\|_2^2 \quad \text{s.t. } \mathbf{x} \in \mathcal{C}_q \cap \mathcal{C}_{\text{FR}} \cap \mathcal{C}_{\text{AC}}, \quad (17)$$

where the feasible space \mathcal{C}_q of \mathbf{x} is restricted by $g(\mathbf{x} | \mathbf{x}^i) \geq P_t$.

The problem (17) is a convex quadratically constrained quadratic program (QCQP) problem and can be efficiently solved by an off-the-shelf convex optimization toolbox, such as CVX [33]. We summarize the whole algorithm in Algorithm 2.

IV. NUMERICAL RESULTS

In this section, we provide the numerical results to demonstrate the validity of our proposed algorithm and the performance gain in FA-assisted ISAC systems. We set the parameters of FAs as $D_0 = \lambda/2$, $D = M\lambda$, and $\lambda = 0.01$ m [19], [34]. In addition, we set $P_{\text{max}} = 30$ dBm, $\sigma^2 = -80$ dBm, $K = 2$, $\sigma_k = g_0 d_k^{-\alpha}$, where $g_0 =$

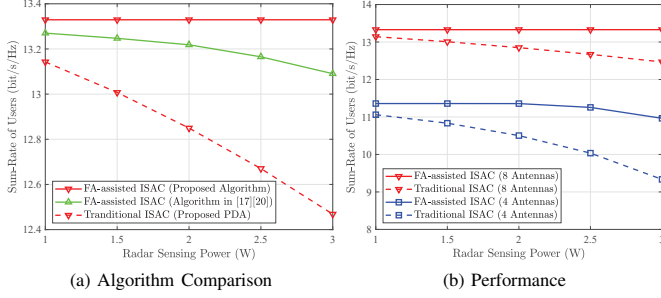


Fig. 2. Sum-rate of users under different radar sensing power.

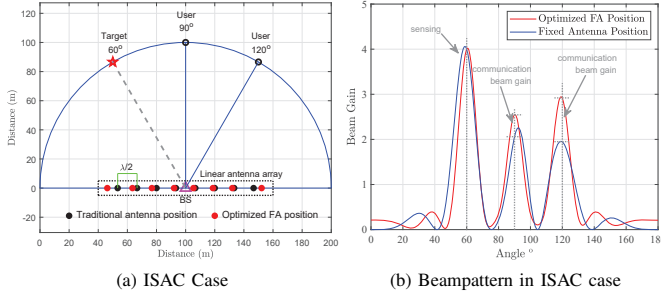


Fig. 3. Case study in FA-assisted ISAC systems.

−40 dB denotes the expected value of the average channel power gain at a reference distance of 1 m, and $\alpha = 2.8$ denotes the path-loss exponent. Users are distributed around BS at a distance of 100 m, which means $d_k = 100$ m for $k = 1, 2, \dots, K$. Moreover, we set $\theta = 60^\circ$, $\theta_1 = 90^\circ$, and $\theta_2 = 120^\circ$. We stop all the algorithms when $\sum_{k=1}^K |\log_2(1 + \gamma_k(\mathbf{W}^{l+1}, \mathbf{x}^{l+1})) - \log_2(1 + \gamma_k(\mathbf{W}^l, \mathbf{x}^l))| \leq 10^{-4}$, and all numerical results are the average over 500 independent trials.

Fig. 2 (a) shows the validity of the proposed algorithm with $M = 8$. The benchmark algorithm is the algorithm in [17], [20]. The average runtimes of the proposed algorithm and the benchmark algorithm are shown in Table I with the different probing power. It can be seen that the average runtimes required for the benchmark algorithms to design the beamformer exceeds 14 seconds, while the average runtime of our proposed algorithm is only within 1 second, which is a significant improvement. Moreover, from Fig. 2 (a), the proposed algorithm owns the superior performance compared to the benchmark algorithm. In other words, our proposed algorithm not only achieves higher performance but also solves more than 15 times faster compared to the benchmark algorithm.

Fig. 2 (b) shows the sum rate of users with different radar sensing power under different antenna numbers. It is obvious that with the enhancement of sensing power, communication performance gradually decreases. Moreover, the 4-antenna system has a faster degradation of communication performance compared to the 8-antenna system as the radar sensing power increases in the target direction. By optimizing the FA positions, the performance degradation trend is slowed down and the stability of communication performance can be ensured

TABLE I
RUNNING TIME COMPARISON

Average Runtime	Algorithm		
		Our Algorithm	[17], [20]
Sensing Power			
$P_t = 1$ W		0.8701 (s)	14.5468 (s)
$P_t = 2$ W		0.8924 (s)	14.5613 (s)
$P_t = 3$ W		0.9191 (s)	14.5808 (s)

to a greater extent in the 8-antenna system. This is due to the higher channel gain that can be achieved by flexibly deploying FAs to improve ISAC performance. In Fig. 3, we provide a case study to illustrate how FAs enhance ISAC performance. We can see that the optimal antenna position is not uniform, and by optimizing FA positions, higher communication beam gain is obtained to improve the channel.

V. CONCLUSION

In this paper, we have considered an FA-assisted ISAC system. By optimizing the beamformer and FA positions, the design aimed to maximize the multiuser sum-rate under the probing power constraint and the total transmission power constraint. The resulting problem is non-convex. We have devised an efficient algorithm to alternatively update the beamformer and FA positions. Numerical results have demonstrated the performance of ISAC systems can be enhanced by the optimized FA positions.

APPENDIX A DERIVATION OF $\tilde{\mathbf{w}}_t$

We can derive $\tilde{\mathbf{w}}_t$ by solving the following problem

$$\min_{\mathbf{w}} \|\mathbf{w} - \boldsymbol{\xi}\|_2^2 \quad \text{s.t.} \quad \sum_{k=1}^K \mathbf{w}_k^H \mathbf{a} \mathbf{a}^H \mathbf{w}_k \geq P_t, \quad (18)$$

where $\boldsymbol{\xi} = [\boldsymbol{\xi}_1^T, \boldsymbol{\xi}_2^T, \dots, \boldsymbol{\xi}_K^T]^T$ is the point to project, and \mathbf{a} denotes $\mathbf{a}(\mathbf{x}, \theta)$ for short.

The Karush–Kuhn–Tucker (KKT) conditions associated with problem (18) are given by

$$\begin{aligned} \frac{\partial \mathcal{L}}{\partial \mathbf{w}_k} &= 2(\mathbf{w}_k - \boldsymbol{\xi}_k) - 2\mu \mathbf{a} \mathbf{a}^H \mathbf{w}_k = 0, \quad k = 1, 2, \dots, K, \\ \sum_{k=1}^K \mathbf{w}_k^H \mathbf{a} \mathbf{a}^H \mathbf{w}_k &\geq P_t, \quad \mu \geq 0, \quad \mu \left(\sum_{k=1}^K \mathbf{w}_k^H \mathbf{a} \mathbf{a}^H \mathbf{w}_k - P_t \right) = 0, \end{aligned}$$

where $\mu \geq 0$ is the dual variable. From the first line of KKT condition and Woodbury matrix identity, we get

$$\mathbf{w}_k^* = (\mathbf{I} - \mu \mathbf{a} \mathbf{a}^H)^{-1} \boldsymbol{\xi}_k = \left(\mathbf{I} + \frac{\mu \mathbf{a} \mathbf{a}^H}{1 - \mu \mathbf{a}^H \mathbf{a}} \right) \boldsymbol{\xi}_k, \quad (19)$$

By the complementary slackness, we know that if $\sum_{k=1}^K \mathbf{w}_k^H \mathbf{a} \mathbf{a}^H \mathbf{w}_k > P_t$, then $\mu = 0$ must hold. Otherwise, μ is chosen such that $\sum_{k=1}^K \mathbf{w}_k^H \mathbf{a} \mathbf{a}^H \mathbf{w}_k = P_t$, given by

$$\mu = \frac{1}{(\mathbf{a}^H \mathbf{a})^2} - \sqrt{\frac{\sum_{k=1}^K \boldsymbol{\xi}_k^H \mathbf{a} \mathbf{a}^H \boldsymbol{\xi}_k}{(\mathbf{a}^H \mathbf{a})^2 P_t}}. \quad (20)$$

The derivation is complete.

REFERENCES

- [1] F. Liu, Y. -F. Liu, A. Li, C. Masouros, and Y. C. Eldar, "Cramér-Rao bound optimization for joint radar-communication beamforming," *IEEE Trans. Signal Process.*, vol. 70, pp. 240–253, Jan. 2022.
- [2] J. A. Zhang et al., "Enabling joint communication and radar sensing in mobile networks—A survey," *IEEE Commun. Surv. Tutorials*, vol. 24, no. 1, pp. 306–345, Firstquarter 2022.
- [3] F. Liu, C. Masouros, A. Li, H. Sun, and L. Hanzo, "MU-MIMO communications with MIMO radar: From co-existence to joint transmission," *IEEE Trans. Wireless Commun.*, vol. 17, no. 4, pp. 2755–2770, Apr. 2018.
- [4] F. Liu, L. Zhou, C. Masouros, A. Li, W. Luo, and A. Petropulu, "Toward dual-functional radar-communication systems: Optimal waveform design," *IEEE Trans. Signal Process.*, vol. 66, no. 16, pp. 4264–4279, Aug. 2018.
- [5] Z. Liao and F. Liu, "Symbol-level precoding for integrated sensing and communications: A faster-than-Nyquist approach," *IEEE Commun. Lett.*, vol. 27, no. 12, pp. 3210–3214, Dec. 2023.
- [6] Y. Chen, F. Liu, Z. Liao, and F. Dong, "Symbol-level precoding for MIMO ISAC transmission based on interference exploitation," *IEEE Commun. Lett.*, vol. 28, no. 2, pp. 283–287, Feb. 2024.
- [7] R. Liu, M. Li, and A. L. Swindlehurst, "Joint beamforming and reflection design for RIS-assisted ISAC systems," in *Proc. 30th Eur. Signal Process. Conf. (EUSIPCO)*. Belgrade, Serbia, 2022, pp. 997–1001.
- [8] Z. Wang, Y. Liu, X. Mu, Z. Ding, and O. A. Dobre, "NOMA empowered integrated sensing and communication," *IEEE Commun. Lett.*, vol. 26, no. 3, pp. 677–681, Mar. 2022.
- [9] Y. Dong, F. Liu, and Y. Xiong, "Joint receiver design for integrated sensing and communications," *IEEE Commun. Lett.*, vol. 27, no. 7, pp. 1854–1858, Jul. 2023.
- [10] Q. Zhu, M. Li, R. Liu, and Q. Liu, "Joint transceiver beamforming and reflecting design for active RIS-aided ISAC systems," *IEEE Trans. Veh. Technol.*, vol. 72, no. 7, pp. 9636–9640, Jul. 2023.
- [11] Z. Xu, F. Liu, and A. Petropulu, "Cramér-Rao bound and antenna selection optimization for dual radar-communication design," in *Proc. IEEE Int. Conf. Acoust., Speech, Signal Process. (ICASSP)*. Singapore, Singapore, 2022, pp. 5168–5172.
- [12] X. Song, J. Xu, F. Liu, T. X. Han, and Y. C. Eldar, "Intelligent reflecting surface enabled sensing: Cramér-Rao bound optimization," *IEEE Trans. Signal Process.*, vol. 71, pp. 2011–2026, Jun. 2023.
- [13] K. Shen and W. Yu, "Fractional programming for communication systems—Part I: Power control and beamforming," *IEEE Trans. Signal Process.*, vol. 66, no. 10, pp. 2616–2630, May 2018.
- [14] K. -K. Wong, W. K. New, X. Hao, K. -F. Tong, and C. -B. Chae, "Fluid antenna system—Part I: Preliminaries," *IEEE Commun. Lett.*, vol. 27, no. 8, pp. 1919–1923, Aug. 2023.
- [15] K. -K. Wong, K. -F. Tong, and C. -B. Chae, "Fluid antenna system—Part III: A new paradigm of distributed artificial scattering surfaces for massive connectivity," *IEEE Commun. Lett.*, vol. 27, no. 8, pp. 1929–1933, Aug. 2023.
- [16] W. Ma, L. Zhu, and R. Zhang, "MIMO capacity characterization for movable antenna systems," *IEEE Trans. Wireless Commun.*, vol. 23, no. 4, pp. 3392–3407, Apr. 2024.
- [17] Y. Ye, L. You, J. Wang, H. Xu, K. -K. Wong, and X. Gao, "Fluid antenna-assisted MIMO transmission exploiting statistical CSI," *IEEE Commun. Lett.*, vol. 28, no. 1, pp. 223–227, Jan. 2024.
- [18] H. Qin, W. Chen, Z. Li, Q. Wu, N. Cheng, and F. Chen, "Antenna positioning and beamforming design for fluid antenna-assisted multi-user downlink communications," *IEEE Wireless Commun. Lett.*, vol. 13, no. 4, pp. 1073–1077, Apr. 2024.
- [19] W. Ma, L. Zhu, and R. Zhang, "Multi-beam forming with movable-antenna array," *IEEE Commun. Lett.*, vol. 28, no. 3, pp. 697–701, Mar. 2024.
- [20] Y. Zuo, J. Guo, B. Sheng, C. Dai, F. Xiao, and S. Jin, "Fluid antenna for mobile edge computing," *arXiv preprint arXiv:2403.11806*, 2024.
- [21] J. Zhu, G. Chen, P. Gao, P. Xiao, Z. Lin, and A. Quddus, "Index modulation for fluid antenna-assisted MIMO communications: System design and performance analysis," *IEEE Trans. Wireless Commun.*, 2024, Early Access.
- [22] D. Zhang, S. Ye, M. Xiao, K. Wang, M. D. Renzo, and M. Skoglund, "Fluid antenna array enhanced over-the-air computation," *IEEE Wireless Commun. Lett.*, 2024, Early Access.
- [23] C. Wang, G. Li, H. Zhang, K. -K. Wong, Z. Li, D. W. K. Ng, and C. -B. Chae, "Fluid antenna system liberating multiuser MIMO for ISAC via deep reinforcement learning," *IEEE Trans. Wireless Commun.*, 2024, Early Access.
- [24] P. Stoica, J. Li, and Y. Xie, "On probing signal design for MIMO radar," *IEEE Trans. Signal Process.*, vol. 55, no. 8, pp. 4151–4161, Aug. 2007.
- [25] Q. Shi, M. Razaviyayn, Z. -Q. Luo, and C. He, "An iteratively weighted MMSE approach to distributed sum-utility maximization for a MIMO interfering broadcast channel," *IEEE Trans. Signal Process.*, vol. 59, no. 9, pp. 4331–4340, Aug. 2011.
- [26] S. Wang, Q. Li, S. X. Wu, and J. Lin, "Sum rate maximization for multiuser MISO downlink with intelligent reflecting surface," *arXiv preprint arXiv:1912.09315*, 2019.
- [27] M. Shao and W. -K. Ma, "A simple way to approximate average robust multiuser MISO transmit optimization under covariance-based CSIT," in *IEEE Int. Conf. Acoustics, Speech Signal Process. (ICASSP)*, 2017, pp. 3504–3508.
- [28] K. L. Keys, H. Zhou, and K. Lange, "Proximal distance algorithms: Theory and practice," *J. Machine Learning Research*, vol. 20, no. 1, pp. 2384–2421, 2019.
- [29] Q. Zhang, M. Shao, Q. Li, and J. Liu, "An efficient algorithm for multiuser sum-rate maximization of large-scale active RIS-aided MIMO system," in *Proc. IEEE Int. Conf. Acoust., Speech, Signal Process. (ICASSP)*. Seoul, Korea, 2024, pp. 9036–9040.
- [30] Q. Li, Y. Liu, M. Shao, and W. -K. Ma, "Proximal distance algorithm for nonconvex QCQP with beamforming applications," in *Proc. IEEE Int. Conf. Acoust., Speech, Signal Process. (ICASSP)*. Barcelona, Spain., 2020, pp. 5155–5159.
- [31] M. Shao, Q. Li, W. -K. Ma, and A. M. -C. So, "A framework for one-bit and constant-envelope precoding over multiuser massive MISO channels," *IEEE Trans. Signal Process.*, vol. 67, no. 20, pp. 5309–5324, Oct. 2019.
- [32] S. Boyd, S. P. Boyd, and L. Vandenberghe, *Convex Optimization*. Cambridge, U.K.: Cambridge Univ. Press, 2004.
- [33] M. Grant and S. Boyd, "CVX: Matlab software for disciplined convex programming, version 2.1 beta," 2014, [Online]. Available: <http://cvxr.com/cvx>.
- [34] L. Zhu, W. Ma, and R. Zhang, "Modeling and performance analysis for movable antenna enabled wireless communications," *IEEE Trans. Wireless Commun.*, 2023, Early Access.